Available online at www.sciencedirect.com
ScienceDirect
Trans. Nonferrous Met. Soc. China 22(2012) 1778−1785
Transactions of Nonferrous Metals Society of China
www.tnmsc.cn

Anodizing of AZ91D magnesium alloy using environmental friendly alkaline borate-biphthalate electrolyte

LIU Yan[1,2], YANG Fu-wei[2], WEI Zhong-ling[3], ZHANG Zhao[1]

1. Department of Chemistry, Zhejiang University, Hangzhou 310027, China;
2. Department of Chemistry, Tianshui Normal University, Tianshui 741000, China;
3. Magnesium Technology Co., Ltd., Chinese Academy of Sciences, Jiaxing 314051, China

Received 19 July 2011; accepted 28 February 2012

Abstract: A kind of environmental friendly anodizing routine for AZ91D magnesium alloy, based on an alkaline borate-potassium acid phthalate (KAP) electrolyte, was studied. The effect of KAP on the properties of the anodized film was investigated by scanning electron microscopy (SEM), X-ray diffraction (XRD), energy dispersive spectrometry (EDS), potentiodynamic polarization and electrochemical impedance spectroscopy (EIS), respectively. The results showed that the anodizing process, surface morphology, thickness, phase structure and corrosion resistance of the anodized film were strongly dependent on the concentration of KAP. In the presence of adequate KAP, a compact and smooth anodized film with excellent corrosion resistance was obtained.
Key words: anodizing; magnesium alloy; potassium acid phthalate; environmental friendly electrolyte; corrosion performance

1 Introduction

Magnesium alloy is becoming one of the most promising metals for lightweight industry because of its specific high strength, high dimensional stability, good electromagnetic shielding and damping characteristics [1]. However, the poor corrosion resistance of magnesium alloy hinders its application especially in corrosive environment [2−4].

To improve the corrosion resistance of magnesium alloy, various technologies including alloying, surface modification, chemical conversion, electroplating, anodic oxidization, physical vapor deposition and plasma electrolytic oxidation (PEO) [5−8] have been developed. Among them, PEO technology is valued by many researchers [9] for the significant properties of the anodized film, such as good adhesion, high corrosion resistance and high hardness [10−12]. Otherwise, environmental harmful inorganics, such as phosphate [13,14], fluoride [15,16] and aluminate [17,18], and toxic organics, such as hexamethylenetetramine [19] and 1H-benzotriazole [20], are still employed in most of the existing PEO processes. Therefore, new PEO process based on environmental-friendly electrolyte is needed.

In this work, an environmental friendly alkaline borate electrolyte using potassium acid phthalate (KAP) as additive was studied for the PEO treatment of AZ91 magnesium alloy. Compared with other additives used in the PEO process, such as phosphate [13,14], fluoride [15,16], aluminate [17,18], hexamethylenetetramine (LD50 of 50 mg/kg, toxic) [19] and 1H-benzotriazole (LD50 of 965 mg/kg, medium toxic) [20], KAP is safe (LD50≥3200 mg/kg, non-toxic) and environmental friendly [21]. The effect of KAP on the properties of the anodized film was investigated by scanning electron microscopy (SEM), X-ray diffraction (XRD), energy dispersive spectrometry (EDS), potentiodynamic polarization and electrochemical impedance spectroscopy (EIS), respectively.

2 Experimental

2.1 Materials and specimen preparation

AZ91D magnesium alloy was employed in this study, and its chemical composition was listed in Table 1. Prior to the PEO treatment, the alloy sheets with dimensions of 10 mm × 10 mm × 1 mm were polished up

Foundation item: Projects (50771092, 21073162) supported by the National Natural Science Foundation of China; Project (08JC1421600) supported by the Science and Technology Commission of Shanghai, China; Project (2008AZ2018) supported by the Science and Technology Bureau of Jiaxing, China
Corresponding author: ZHANG Zhao; Tel: +86-571-87952318; E-mail: zhangzhao@zju.edu.cn
DOI: 10.1016/S1003-6326(11)61387-3

to 2000 grit, degreased with acetone, and washed with distilled water successively. An AC power supply (120 V, 50 Hz) was employed and the duration of the PEO process was 3 min. The basic anodizing electrolyte was composed of 60 g/L NaOH, 25 g/L $Na_2B_4O_7$ and 20 g/L H_3BO_3. 0−6.0 g/L KAP (its chemical structural formula is shown in Fig. 1) was used as additive. During the anodizing process, the temperature was controlled at 30 °C by a refrigerant equipment (model YT-8A, China). SEM and EDX (SIRION, FEI Company, made in Holland) were utilized to examine the corrosion morphologies and composition of the anodized films. The phase structures of the anodized films were determined with a X-ray diffractometer (XRD, AXS D8 ADVANCE, Bruker company, made in German), using Cu K_α (1.5418 Å) radiation source. The film thickness was measured with a coating thickness measurer (TT240, Beijing Shidai Company, China). The surface roughness (R_a) of the films was measured using a stylus type surface profilometer (E34-001, Haebin, China).

Table 1 Chemical composition of AZ91D magnesium alloy (mass fraction, %)

Al	Zn	Mn	Si	Cu	Ni	Fe	Mg
8.3−9.7	0.35−1.0	0.15−0.50	≤0.01	≤0.030	≤0.002	≤0.005	Bal.

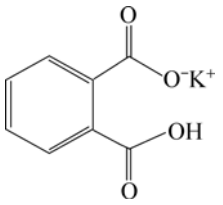

Fig. 1 Chemical structural formula of potassium acid phthalate (KAP)

2.2 Electrochemical set up

Except the anodized film, the other part of the sample was coated with paraffin wax before electrochemical test. During the electrochemical test, the electric contacting was to the magnesium alloy substrate. A three-electrode cell with the anodized film as working electrode, saturated calomel electrode as reference electrode, and platinum sheet as counter electrode was employed in all the tests. The ratio of volume of neutral 3.5% NaCl solution (pH=7.03) to sample area was 50 mL/cm^2. Potentiodynamic polarization test was carried out by a CHI 630D potentiostat (Chenhua, China) at (25±1) °C. The scans were conducted at a rate of 1 mV/s from −0.25 V to 0.75 V (versus open circuit potential (OCP)). Electrochemical impedance spectrum (EIS) was measured at the OCP using an impedance measurement unit (IM6e, Germany) over the frequency range of 0.01−10000 Hz with a voltage amplitude of 5 mV in the neutral 3.5% NaCl solution.

3 Results and discussion

3.1 Effects of KAP on PEO process

Figure 2 shows current density vs time curves during the PEO process in the borate electrolyte with and without KAP. Based on the slopes of current density vs time curves, the anodized growth process can be divided into two stages [22].

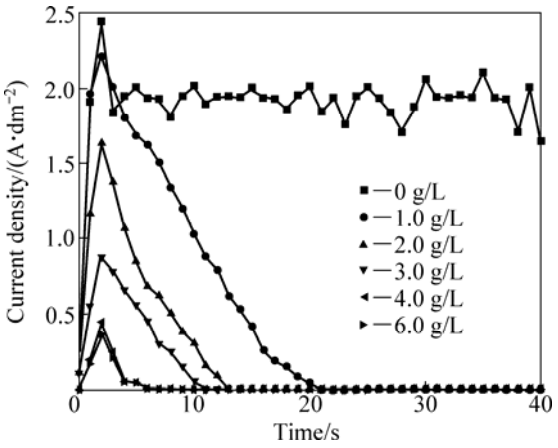

Fig. 2 Variations of current density with time during PEO process in electrolyte with and without KAP

At the first stage, the current density increases gradually and then reaches its maximum value. In the absence of KAP, the current density changes dramatically, and violent sparking and gas release can be observed on the surface of magnesium alloy. However, in the presence of KAP, the increase of current density is obviously suppressed, and it seems that the more the KAP in the electrolyte is, the less the change of the current density is. Nonetheless, when there is more than 4.0 g/L KAP in the electrolyte, the current density is not affected any more. Besides, in the presence of KAP, sparking and gas release can still be observed, but the intensities of them are weakened evidently. At the second stage, the current density decreases gradually until a plateau reaches. The change of the current density is also dependent on the concentration of KAP. The more the KAP in the electrolytes is, the less the change of current density is. During this period, vigorous sparking and gas evolvement can be observed in the absence of the KAP. In the presence of KAP, however, they are inhibited obviously.

Current density not only has a strong dependence on the KAP concentration but also gives back the growth process of anodized film in the electrolyte directly. Excessive high current density often results in inferior PEO coating [23−25], while too low current density makes the formation of the anodized films too slow or

even unachievable [26,27]. In this study, with the addition of KAP in the electrolyte, the current density of the PEO process is reduced and the vigorous sparking and gas evolvement are inhibited. This kind of PEO process at a moderate current density facilitates the improvement of current efficiency [28] and the quality of the anodized film [29].

3.2 Morphology of anodized films

Figure 3 illustrates the surface morphology of the anodized films fabricated on magnesium alloys by PEO process in the basic anodizing electrolyte without and with KAP addition. In the electrolyte without KAP, the resultant anodized film (Fig. 3(a)) is loose and coarse. There are many large-sized chunks, pores and cracks on the surface of the film. However, in the presence of KAP, the large-sized chunks and pores decrease, the cracks disappear, and the anodized films become compact and smooth (Figs. 3(b), (c) and (d), where the concentrations of KAP are 2.0, 4.0 and 6.0 g/L, respectively).

With the increase of the KAP concentration, the roughness of the films decreases gradually (Fig. 4). These results are consistent with the ones from SEM observation. The toughness of the film is closely related with the current density in the PEO process [30]. In the absence of KAP, the current density of the PEO process is very high. Excessive high current density usually leads to large sized chunks, pores and cracks on the anodized film [31−33]. These chunks, pores and cracks are responsible for the increased surface roughness [34,35]. In the presence of KAP, the current density is reduced and the PEO process becomes moderate. Moderate PEO process is helpful for the formation of compact and smooth anodized film [36].

3.3 Phase structure analysis

Figure 5 shows that the films are mainly composed of O, Mg as well as a trace of Al and Na. Mg and Al come from the magnesium alloy substrate. Na is from sodium hydroxide. Besides, in the presence of KAP, the resultant anodized film has more O, Al and less Mg (Table 2), which suggests a better corrosion resistance performance [37].

XRD patterns of the anodized films with different KAP concentrations are shown in Fig. 6. The anodized films consist mainly of MgO and Mg, in accordance with the results of the EDS. MgO is the result of the PEO process. The diffraction peaks of Mg, however, are from the magnesium alloy substrate. With the increase of the KAP concentration (0−4.0 g/L), the intensity of MgO peaks becomes strong. The intensity of Mg peaks, however, decreases gradually and almost disappears when there is more than 4.0 g/L KAP in the electrolyte.

3.4 Thickness of anodized film

Thickness evolution of the anodized film is listed in Table 3. In the absence of KAP, the anodized film has the largest thickness. In the presence of KAP, the thickness of the films reduces slightly over the concentration range of 0−4.0 g/L. When there is more than 4.0 g/L KAP in the electrolyte, the film thickness begins to stabilize. The thickness of the anodized film associates closely with the anodizing current density [38]. In the absence of KAP additive, the anodizing current density is high. High

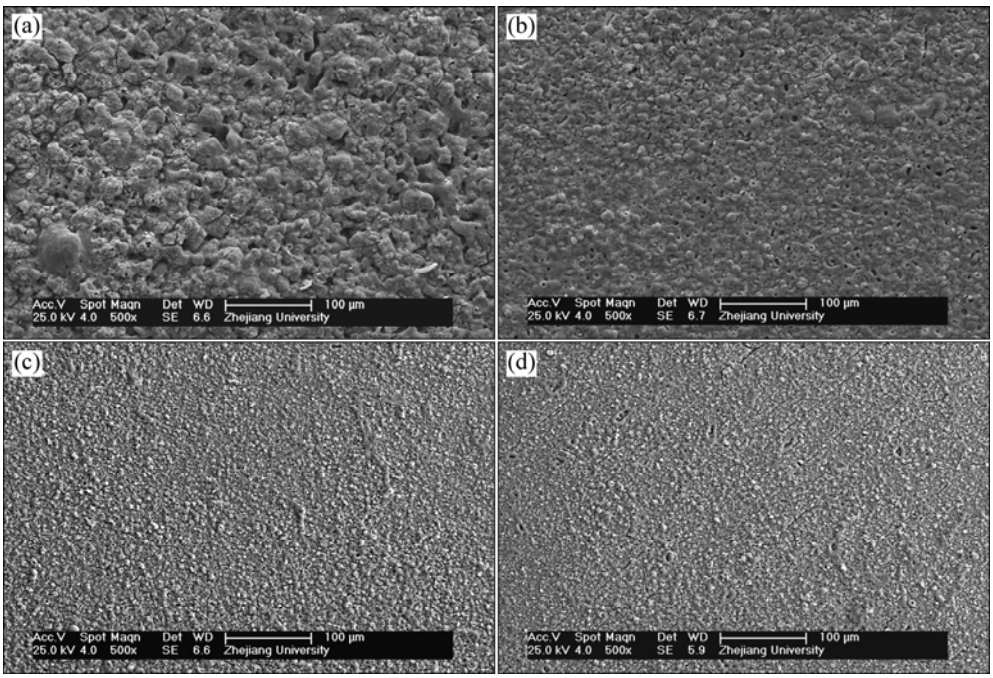

Fig. 3 Surface morphologies of anodized film formed in electrolyte with 0 (a), 2.0 g/L (b), 4.0 g/L (c) and 6.0 g/L (d) KAP

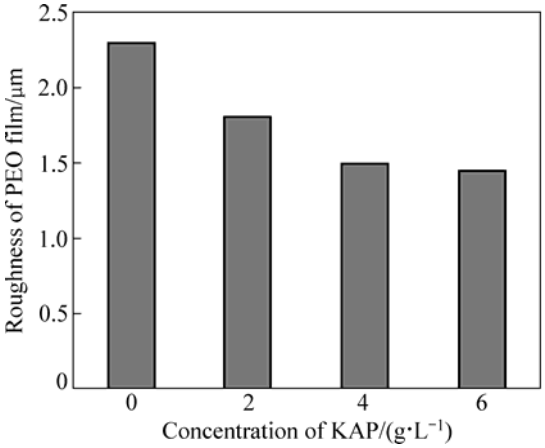

Fig. 4 Roughness of anodized films formed in electrolyte with 0−6.0 g/L of KAP

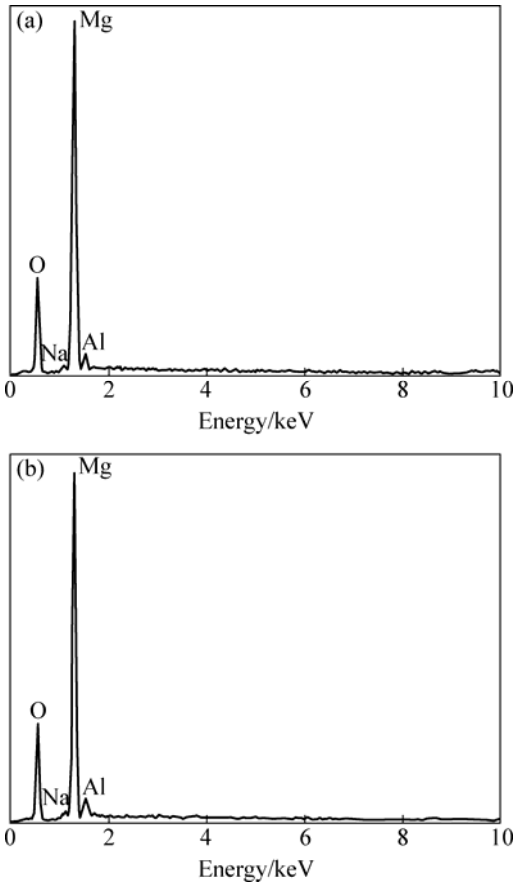

Fig. 5 EDS spectra of anodized film formed in electrolyte with KAP: (a) 0 g/L; (b) 6.0 g/L

Table 2 EDS results of anodized films formed in electrolyte with 0−6.0 g/L of KAP

ρ_{KAP}/(g·L^{-1})	Composition/%			
	O	Na	Mg	Al
0.0	35.80	1.58	56.53	6.09
6.0	36.11	1.58	55.71	6.60

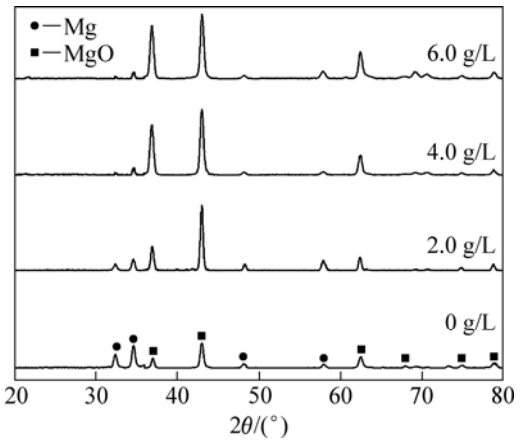

Fig. 6 XRD patterns of anodized films formed in electrolyte with 0−6.0 g/L of KAP

Table 3 Thickness of anodized films formed in electrolyte with 0−6.0 g/L of KAP

ρ_{KAP}/(g·L^{-1})	Average thickness/μm
0.0	39.18
1.0	33.13
2.0	29.15
3.0	27.45
4.0	23.13
5.0	23.02
6.0	23.07

current density can increase the growth rate and thickness of the anodized film [33,39]. However, excessive high current density usually results in loose and porous anodized film [40,41]. In the presence of KAP, the current density is reduced and the PEO process becomes moderate. The resultant anodized film tends to thin, but it usually has more uniform and compact structure [42].

3.5 Corrosion resistance of anodized film

Figure 7 and Table 4 shows the results of the potentiodynamic polarization of the anodized films formed in the solutions with and without KAP. Corrosion current density (J_{corr}), corrosion potential (φ_{corr}) and polarization resistance (R_p) are used to evaluate the corrosion protective property of the anodized films. φ_{corr} and J_{corr} are from the potentiondynamic polarization curves. R_p can be calculated by the following formula [43]:

$$R_p = \frac{\beta_a \beta_c}{2.303 J_{corr}(\beta_a + \beta_c)} \quad (1)$$

where β_a and β_c are anodic and cathodic Tafel slopes, respectively. For the anodized film prepared in the electrolyte without KAP, φ_{corr}, J_{corr} and R_p are −1.502 V,

3.092×10^{-6} A/cm^2 and 1.389×10^{4} Ω·cm^2, respectively. For the anodized films prepared in the electrolyte with 0−4.0 g/L KAP, φ_{corr} is shifted to the positive direction (Fig. 7), J_{corr} is reduced, and R_p is increased (Table 4). The more the KAP in the electrolyte is, the more the improvements of these parameters are. For the anodized films prepared in the electrolyte with 4.0 g/L KAP, φ_{corr}, J_{corr} and R_p are −1.372 V, 2.001×10^{-7} A/cm^2 and 1.618×10^{5} Ω·cm^2, respectively (Table 4). This means a large enhancement in the corrosion protection performance [17].

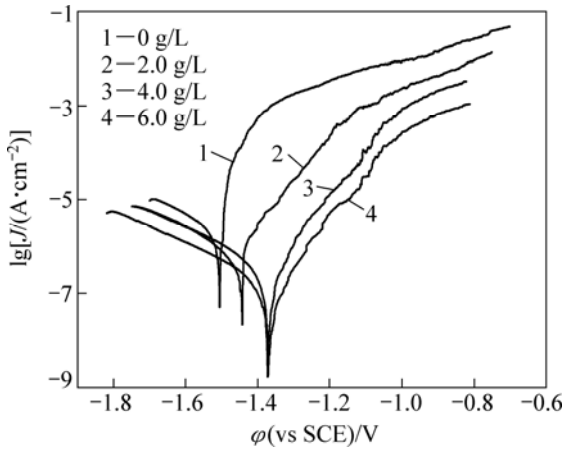

Fig. 7 Potentiodynamic polarization curves of anodized films formed in electrolyte with 0−6.0 g/L KAP

Table 4 Results of potentiodynamic polarization curves for films formed in solutions with KAP

ρ_{KAP}/(g·L^{-1})	φ_{corr}/V	β_a/(mV·dec^{-1})	β_c/(mV·dec^{-1})	R_p/(Ω·cm^2)	J_{corr}/(A·cm^{-2})
0.0	−1.502	185.74	211.60	1.389×10^{4}	3.092×10^{-6}
2.0	−1.443	179.16	118.16	1.552×10^{4}	1.992×10^{-6}
4.0	−1.372	184.47	125.16	1.618×10^{5}	2.001×10^{-7}
6.0	−1.375	169.75	131.23	1.584×10^{5}	2.028×10^{-7}

Figure 8 shows Nyquist, Z_{mod} Bode and phase angle Bode diagrams of anodized films. As shown in Fig. 8(a), there are low-frequency inductive loops for the anodized films prepared in the electrolyte with low concentrations of KAP. This is caused by the pitting corrosion of the aggressive Cl^- in the electrolyte [14]. With the increase of KAP concentration, the diameter of the capacitive loop increases obviously (Fig. 8(a)), indicating the enhancement of the anticorrosion performance of the anodized films. When the concentration of KAP is more than 2.0 g/L, the diameter of the capacitive loop ceases to expand, indicating that the best anticorrosion performance has been achieved. Z_{mod} Bode diagrams in Fig. 8(b) can also be used to estimate the corrosion protection of the anodized films, and the results are in accordance with the results of the Nyquist diagrams.

For the anodized films prepared in the solution containing 0−2.0 g/L KAP, a low frequency capacitive arc and a high frequency capacitive arc are observed in the phase angle Bode diagram (Fig. 8(c)). The corrosion resistance of the anodized film can be also estimated quantitatively by simulating the experimental Bode diagrams using an equivalent circuit (Fig. 9(a)). The equivalent circuit is composed of two time constants in series with anodic film impedance and film/solution impedance. In this equivalent circuit, R_1 represents the electrolyte resistance; R_2 and CPE_1 represent the resistance and capacitance of the anodized film; R_3 and CPE_2 correspond to the charge transfer resistance and the double layer capacitance of film/solution, respectively. The values of the fitting circuit elements are summarized in Table 5. CPE_1-T represents capacitance of the anodized film. CPE_2-T is corresponding to the double layer capacitance of film/solution. CPE_1-P and CPE_2-P reflect the deviation between double layer capacitance of anodized film, film/solution and the pure capacitance, respectively.

The anodized films prepared in the electrolyte with more than 2.0 g/L KAP, however, have only a high frequency capacitive arc, and the capacitive arc of low frequency is not detected. The compact structure and good adhesion of the anodized films prepared in the electrolyte with more than 2.0 g/L KAP, improve the corrosion resistance. This indicates that these anodized films have excellent corrosion resistance to NaCl solution. Thus, the impedance features of the anodized film prepared in the electrolyte with 0−2.0 g/L and more than 2.0 g/L KAP are different. As seen from the equivalent circuit in Fig. 9(b), the impedance measured system consists of three parts: electrolyte, anodized film and metal/electrolyte interface. R_s is the resistance of the solution, CPE represents the double layer capacitance, and R_t is the charge transfer resistance of the anodic film. The impedance parameters derived from the plots are given in Table 6. CPE-T represents the capacitance of anodized film. CPE-P reflects the deviation between the double layer capacitance of anodized film and the pure capacitance. R_t increases with the increase of KAP concentration, which is the same with the change of R_p in

Table 5 Typical impedance data of anodized films formed in electrolyte with 0−2.0 g/L of KAP

ρ_{KAP}/(g·L^{-1})	R_1/(Ω·cm^2)	CPE_1-T/(μF·cm^{-2})	CPE_1-P	R_2/(Ω·cm^2)	CPE_2-T/(μF·cm^{-2})	CPE_2-P	R_3/(Ω·cm^2)
0.0	28.38	2.931	0.867	10384	90.46	0.987	14600
1.0	28.78	2.584	0.854	12376	79.31	0.818	19371

Table 6 Typical impedance data of anodized films formed in electrolyte with 4.0−6.0 g/L KAP

ρ_{KAP}/ (g·L^{-1})	R_s/ (Ω·cm^2)	CPE-T/ (μF·cm^{-2})	CPE-P	R_t/ (Ω·cm^2)
4.0	48.91	0.191	0.866	96203
6.0	46.18	0.187	0.882	97315

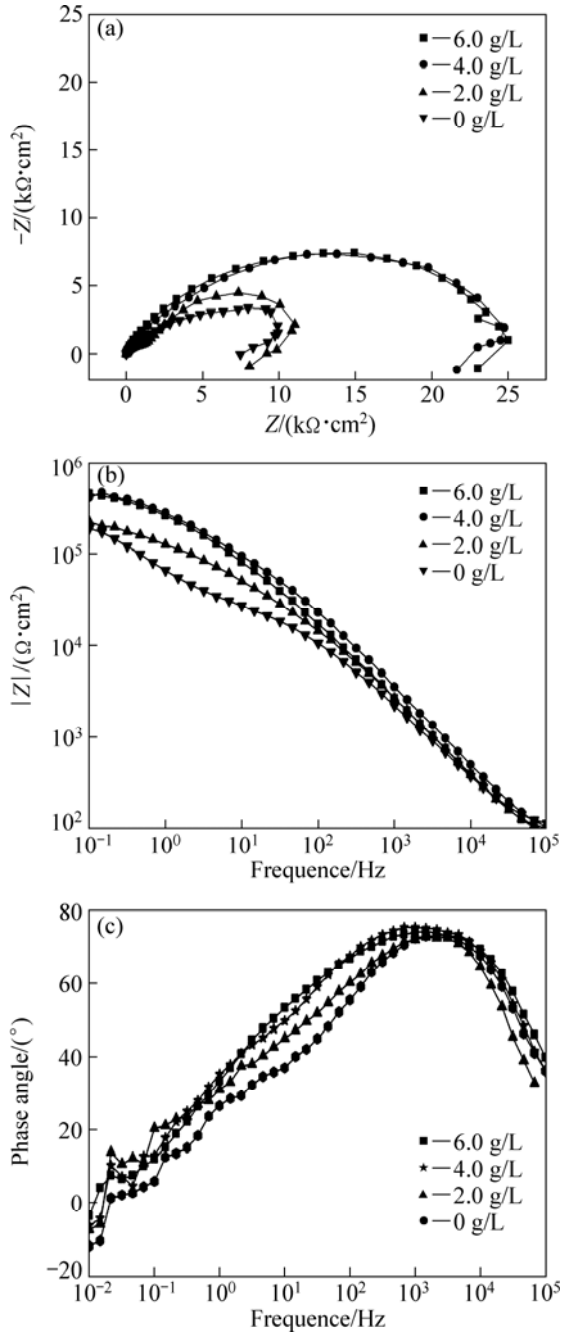

Fig. 8 EIS diagrams for anodized films formed in electrolyte with 0−6.0 g/L of KAP

Table 4. The larger the R_t is, the better the corrosion resistance of the film will be. The corrosion resistance of the anodized film becomes stabilized when the concentration of KAP is more than 2.0 g/L. These results agree well with the ones of the potentiodynamic polarization.

AP^- can adsorb on the surface of magnesium alloy as a kind of hard base, where is rich in Mg^{2+} (hard acid), and form an adsorption layer on the surface of magnesium alloy. The adsorption layer of AP^- leads to the increase of surface resistance and the decrease of the current density of the PEO process subsequently [27]. Moderate sparking at a low current density, however, can eliminate pit ablation [44] and facilitate the formation of the anodized film with high quality—more uniform and compact in structure, stronger in adhesion to the magnesium alloy substrate and better in corrosion resistance.

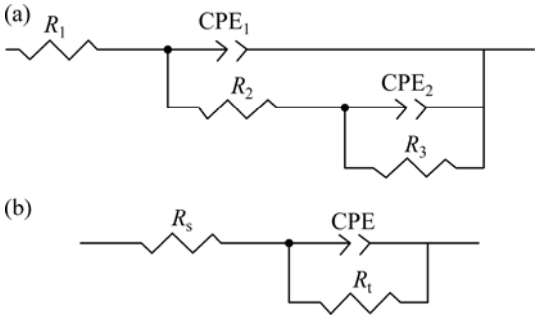

Fig. 9 Equivalent circuit used for simulating behavior of anodized films formed in electrolyte with 0−2.0 (a), and 4.0−6.0 g/L (b) of KAP

4 Conclusions

The anodized films were prepared by plasma electrolytic oxidation (PEO) on AZ91D magnesium alloy in the alkaline borate electrolyte with and without the addition of KAP. The result showed that the PEO process was strongly dependent on the concentration of KAP. In the presence of KAP, the violent sparking and gas release were restrained, and a moderate and controllable PEO condition was obtained. In the presence of adequate KAP, the quality of the anodized film was greatly improved. Anodized films with compact structure, smooth appearance and good adhesion were prepared. Electrochemical testing results showed that this kind of anodized film was excellent in corrosion resistance.

References

[1] GRAY J E, LUAN B. Protective coatings on magnesium and its alloys—A critical review [J]. J Alloy Compd, 2002, 336(1−2): 88−113.

[2] MORDIKE B L, EBERT T. Magnesium properties—Applications potential [J]. Mater Sci Eng, 2001, 302(1): 37−45.

[3] YEROKHIN A L, NIE X, LEYLAND A, MATTHEWS A, DOWEY S J. Plasma electrolysis for surface engineering [J]. Surf Coat Tech, 1999, 122(2): 73−93.

[4] SONG Guang-lin. Recent progress in corrosion and protection of magnesium alloys [J]. Adv Eng Mater, 2005, 7(7): 563−586.

[5] ZHANG Rong-fu, SHAN Da-yong, HAN En-hou, ZENG Zhi-liang. Status and prospect of anodization on magnesium and its alloys [J]. The Chinese Journal of Nonferrous Metals, 2006, 16(7): 1136−1148. (in Chinese)

[6] JIANG Bai-ling, ZHANG Shu-feng, WU Guo-jian, LEI Ting-quan. Micro-flaw and phases constitution of ceramiccoating formed by micro-arc oxidation on magnesium alloys and their influence on corrosion resistance [J]. The Chinese Journal of Nonferrous Metals, 2002, 12(3): 454−457. (in Chinese)

[7] ZHANG Li-jun, ZHANG Zhao, ZHANG Jian-qing. Corrosion behavior of anodized AZ91D magnesium alloy in NaCl aqueous solution [J]. Acta Phys-Chim Sin, 2008, 24(10): 1831−1838. (in Chinese)

[8] YU Gang, LIU Yue-long, LI Ying, YE Li-yuan, GUO Xiao-hua, ZHAO Liang. Corrosion and protection of magnesium alloys [J]. The Chinese Journal of Nonferrous Metals, 2002, 12(6): 1087−1098. (in Chinese)

[9] ZHANG Rong-fa, XIANG Jun-huai, CHAO Qiang-hua, DUO Shu-wang, LI Ming-sheng, LI Wen-kui, HE Xiang-ming, HU Chang-yuan. Effects of $C_6H_{18}O_{24}P_6$ on properties of microarc coatings formed on AZ91HP magnesium alloy in Na_2SiO_3 electrolyte [J]. Transactions of Nonferrous Metals Society of China, 2007, 17(s1): s789−s793.

[10] LALEH M, SABOUR A, SHAHRABI T, SHANGHI A. Effect of alumina sol addition to micro-arc oxidation electrolyte on the properties of MAO coatings formed on magnesium alloy AZ91D [J]. J Alloy Compd, 2010, 496(1): 548−552.

[11] HAO Jian-min, CHEN Hong, ZHANG Rong-jun, JIANG Bai-ling. Corrosion resistance of magnesium alloys micro-arc oxidation ceramic coating [J]. The Chinese Journal of Nonferrous Metals, 2003, 13(4): 988−991. (in Chinese)

[12] CAI Q Z, WANG L S, WEI B K, LIU Q X. Electrochemical performance of microarc oxidation films formed on AZ91D magnesium alloy in silicate and phosphate electrolytes [J]. Surf Coat Tech, 2006, 200(12−13): 3727−3733.

[13] LUO Hai-he, CAI Qi-zhou, WEI Bo-kang, YU Bo, HE Jian, LI Ding-jun. Effect of $(NaPO_3)_6$ on electrochemical corrosion characteristic of micro-arc oxidat ion ceramic coatings formed on AZ91D Mg alloy [J]. Acta Phys Chim Sin, 2008, 24(3): 481−486. (in Chinese)

[14] WANG Li, CHEN Li, YAN Zong-cheng, WANG Hong-lin, PENG Jia-zhi. The influence of additives on the stability behavior of electrolyte, discharges and PEO films characteristics [J]. J Alloys Compd, 2010, 493(1−2): 445−452.

[15] WANG L, CHEN L, YAN Z C, WANG H L, PENG J Z. Effect of potassium fluoride on structure and corrosion resistance of plasma electrolytic oxidation films formed on AZ31 magnesium alloy [J]. J Alloys Compd, 2009, 480(2): 469−474.

[16] CHENG Ying-liang, WU Hai-lan, CHEN Zhen-hua, WANG Hui-min, ZHANG Zhao, WU You-wu. Corrosion properties of AZ31 magnesium alloy and the protective effects of chemical conversion layers and anodized coatings [J]. Transaction of Nonferrous Metals Society of China, 2007, 17(3): 502−508.

[17] LI Y C, YU X, ZHI H Y, WANG Y Y, MASAZUMI O. Anodizing of magnesium alloy AZ31 in alkaline solutions with silicate under continuous sparking [J]. Corros Sci, 2008, 50(12): 3274−3279.

[18] WEN Q, CAO F H, SHI Y Y, ZHANG Z, ZHANG J Q. The effect of phosphate on MAO of AZ91D magnesium using AC power source [J]. Mater Corros, 2008, 59 (10): 819−824.

[19] BAI A, CHEN Z. Effect of electrolyte additives on anti-corrosion ability of micro-arc oxide coatings formed on magnesium alloy [J]. Surf Coat Technol, 2009, 203(14): 1956−1963.

[20] GUO X H, AN M Z, YANG P X, LI H X, SU C N. Effects of benzotriazole on anodized film formed on AZ31B magnesium alloy in environmental-friendly electrolyte [J]. J Alloys Compd, 2009, 482(1−2): 487−497.

[21] EMS-MSDS-IB-093. Material safety data sheet [S].

[22] WU X H, PEI B SU, ZHAO H J, SONG M. Influences of current density on tribological characteristics of ceramic coatings on ZK60 Mg alloy by plasma electrolytic oxidation [J]. Appl Mater Interfaces, 2010, 2(3): 808−812.

[23] WU C S, ZHANG Z, CAO F. H, ZHANG J Q, CAO C N. Study on anodizing of AZ31 magnesium alloys in alkaline borate solutions [J]. Appl Surf Sci, 2007, 253(8): 3893−3898.

[24] BARCHICHE C E, ROCCA E, JUERS C, HAZAN J, STEINMETZ. Corrosion resistance of plasma-anodized AZ91D magnesium alloy by electrochemical methods [J]. J Electrochim Acta, 2007, 53(2): 417−425.

[25] LI M J, TAMURA T, OMURA N, MIWA K. Effects of magnetic field and electric current on the solidification of AZ91D magnesium alloys using an electromagnetic vibration technique [J]. J Alloys Compd, 2009, 487(1−2): 187−193.

[26] SHI Z M, SONG G L, ATRENS A. Influence of anodising current on the corrosion resistance of anodised AZ91D magnesium alloy [J]. Corros Sci, 2006, 48(9): 1939−1959.

[27] KHASELEV O, WEISS D, YAHALOM. Structure and composition of anodic films formed on binary Mg–Al alloys in KOH–aluminate solutions under continuous sparking [J]. Corros Sci, 2001, 43(7): 1295−1307.

[28] LÜ Wei-ling, MA Ying, CHEN Ti-jun, XU Wei-jun, YANG Jian, HAO Yuan. Effects of oxidation time on microstructures and properties of micro-arc oxidation coatings of AZ91D magnesium alloy [J]. The Chinese Journal of Nonferrous Metals, 2009 19(8): 1385−1390. (in Chinese)

[29] WU H L, CHENGY L, LI L L, CHEN Z H, WANG H M, ZHANG Z. The anodization of ZK60 magnesium alloy in alkaline solution containing silicate and the corrosion properties of the anodized films [J]. Appl Surf Sci, 2004, 253(24): 9387−9394.

[30] LIANG J, HU L T, HAO J C. Improvement of corrosion properties of microarc oxidation coating on magnesium alloy by optimizing current density parameters [J]. Appl Surf Sci, 2007, 253(16): 6939−6945.

[31] BALA S P, LIANG J, BLAWERTl C, STORMER M, DIETZEL W. Effect of current density on the microstructure and corrosion behaviour of plasma electrolytic oxidation treated AM50 magnesium alloy [J]. Appl Surf Sci, 2009, 255(7): 4212−4218.

[32] VERDIER S, BOINET M, MAXIMOVITCH S, DALARD F. Formation, structure and composition of anodic films on AM60 magnesium alloy obtained by DC plasma anodizing [J]. Corros Sci, 2005, 47(6): 1429−1444.

[33] GUO H F, AN M Z, XU S, HUO H B. Formation of oxygen bubbles and its influence on current efficiency in micro-arc oxidation process of AZ91D magnesium alloy [J]. Thin Solid Film, 2005, 485(1−2): 53−58.

[34] WANG Y H, WANG J, ZHANG J B, ZHANG Z. Effects of spark discharge on the anodic coatings on magnesium alloy [J]. Matter Lett, 2006, 60(4): 474−478.

[35] LEE Y K, LEE K S, JUNG T. Study on microarc oxidation of AZ31B magnesium alloy in alkaline metal silicate solution [J]. Electrochem Commun, 2008, 10(11): 1716−1719.

[36] CHAI L Y, YU X, YANG Z H, WANG Y Y, OKIDO M. Anodizing of magnesium alloy AZ31 in alkaline solutions with silicate under continuous sparking [J]. Corros Sci, 2008, 50(12): 3274−3279.

[37] CAO F H, ZHANG Z, ZHANG J Q, CAO C N. Plasma electrolytic oxidation of AZ91D magnesium alloy with different additives and its corrosion behavior [J]. Mater Corros, 2007, 58(9): 696−703.

[38] ZHANG Y J, YAN C W, WANG F H, LOU H Y, CAO C N. Study on the environmentally friendly anodizinig of AZ91D magnesium alloy

[J]. Surf Coat Technol, 2002, 161(1): 36−43.

[39] ZHANG R F, SHAN D Y, CHEN R S, HAN E H. Effects of electric parameters on properties of anodic coatings formed on magnesium alloys [J]. Mater Chem Phys, 2008, 107(18): 356−363.

[40] VERDIER S, BOINET M, MAXIMOVITCHS, DALARD F. Formation, structure and composition of anodic films on AM60 magnesium alloy obtained by DC plasma anodizing [J]. Corros Sci, 2005, 47(6): 1429−1444.

[41] BOINET M, VERDIER S, MAXIMOVITCH S, DALARD F. Plasma electrolytic oxidation of AM60 magnesium alloy: Monitoring by acoustic emission technique. Electrochemical properties of coatings [J]. Surf Coat Technol, 2005, 199(2−3): 141−145.

[42] BLAWERT C, DIETZEL W, GHALI E, SONG G. Anodizing treatments for magnesium alloys and their effect on corrosion resistance in various environments [J]. Adv Eng Mater, 2006, 8(6): 511−533.

[43] STERN M, GEARY A L. Electrochemical polarization (I): A theoretical analysis of the shape of polarization curves [J]. J Electrochem Soc, 1957, 104(1): 56−63.

[44] HUSSEIN R O, NIE X, NORTHWOOD D O. Influence of process parameters on electrolytic plasma discharging behaviour and aluminum oxide coating microstructure [J]. Surf Coat Technol, 2010, 205(6): 1659−1667.

邻苯二甲酸氢钾−硼酸盐电解液中 AZ91D 镁合金的阳极氧化

刘 妍[1,2]，杨富巍[2]，卫中领[3]，张 昭[1]

1. 浙江大学 化学系，杭州 310027；
2. 天水师范学院 化学系，天水 741000；
3. 中国科学院 镁合金技术中心，嘉兴 314051

摘 要：研究 AZ91D 镁合金在邻苯二甲酸氢钾−硼酸盐碱性环保型电解液中的阳极氧化行为。考察邻苯二甲酸氢钾对阳极氧化膜层性能的影响，并利用扫描电镜(SEM)、X 射线衍射(XRD)、动电位极化和电化学阻抗(EIS)进行分析表征。结果表明，邻苯二甲酸氢钾的浓度对阳极氧化成膜过程，氧化膜的表面形貌、厚度、相结构和耐腐蚀性能都有重要影响。在硼酸盐电解液中加入适量的邻苯二甲酸氢钾以后，制得的阳极氧化膜表面光滑、致密，与镁合金基体的结合力强，具有优异的耐腐蚀性能。

关键词：阳极氧化；镁合金；邻苯二甲酸氢钾；环保型电解液；腐蚀性能

(Edited by YANG Hua)